*Geological Magazine*

**www.cambridge.org/geo**

## Original Article

**Cite this article:** Florez-Amaya SL, Abdullin F, Bedoya A, Maldonado R, Milián de la Cruz RE, Solari L, Solé J, and Ortega-Obregón C (2023) Detecting the Laramide event in southern Mexico by means of apatite fission-track thermochronology. *Geological Magazine* **160**: 322–333. https://doi.org/10.1017/S0016756822000929

Received: 3 February 2022
Revised: 11 August 2022
Accepted: 17 August 2022
First published online: 23 November 2022

**Keywords:**
Mexico; Sierra Madre del Sur; Late Cretaceous; Eocene; exhumation; apatite fission-track analysis

**Author for correspondence:**
Fanis Abdullin,
Email: fanis@geociencias.unam.mx



# Detecting the Laramide event in southern Mexico by means of apatite fission-track thermochronology

Sandra Lorena Florez-Amaya[1], Fanis Abdullin[2], Alejandra Bedoya[1], Roberto Maldonado[3], Ricardo Enrique Milián de la Cruz[1], Luigi Solari[4], Jesús Solé[5] and Carlos Ortega-Obregón[4]

[1]Posgrado en Ciencias de la Tierra, Centro de Geociencias, Campus Juriquilla, Universidad Nacional Autónoma de México, Querétaro 76230, Mexico; [2]CONACyT–Centro de Geociencias, Campus Juriquilla, Universidad Nacional Autónoma de México, Querétaro 76230, Mexico; [3]Instituto de Geología, Universidad Nacional Autónoma de México, Ciudad Universitaria, Mexico City 04510, Mexico; [4]Centro de Geociencias, Campus Juriquilla, Universidad Nacional Autónoma de México, Querétaro 76230, Mexico and [5]LANGEM–Instituto de Geología, Universidad Nacional Autónoma de México, Ciudad Universitaria, Mexico City 04510, Mexico

## Abstract

In this study, we present apatite fission-track results obtained for ten rock samples collected from three different areas across the Sierra Madre del Sur, southern Mexico. The central objective of our study is the timing of the exhumation event that took place in southern Mexico during Late Cretaceous–Palaeogene time. The thermochronometric data obtained during this work indicate that a Late Cretaceous–Eocene cooling is recorded within the Sierra Madre del Sur, and this is interpreted as resulting from exhumation, an orogenic event that is contemporaneous with the Laramide *sensu lato* (or the Mexican Orogeny). The fission-track ages become younger from west to east across the Sierra Madre del Sur, whereas the cooling rates also increased in the same direction approximately during Campanian–middle Eocene time. Here, we suggest that the activity of the major fault systems of southern Mexico, such as the Caltepec and the Oaxaca faults, played a primary role in the development of geological structures and the exhumation of the Sierra Madre del Sur. Active magmatism during the evolution of the Mexican Orogen implicates the subducted Farallon slab as the main driver of crustal thickening. Moreover, the possible influence of the eastward movement of the Chortis Block on the deformation of the Sierra Madre del Sur cannot be ruled out.

## 1. Introduction and objective

During Late Cretaceous and Palaeogene times, the continental interior of Mexico was affected by the Mexican Orogeny (a term recently introduced by Fitz-Díaz *et al.* 2018), an orogenic activity also known as the Laramide *sensu lato* (e.g. Garduño-Martínez *et al.* 2015). The Mexican Orogen is a large tectonic province that has a spectacular topographic expression in the Sierra Madre Oriental and the Sierra Madre del Sur (Fig. 1). The shortening deformation encompassed the entire modern crustal domain lying between the Pacific Ocean and the Gulf of Mexico. This orogen has a length of more than 2000 km and is hundreds of kilometres wide along a territory that extends northward from the Tehuantepec Isthmus in Oaxaca to northeastern Sonora (Fig. 1). The geological structures in the foreland of the Mexican Orogen have a general NW–SE trend in central Mexico that changes to E–W in northeastern Mexico at the Monterrey salient and back again to NW–SE in northwestern Mexico at the Torreón re-entrant (Fig. 1). Several authors (e.g. Campa & Coney, 1983; Nieto-Samaniego *et al.* 2006; Cerca *et al.* 2007; Cuéllar-Cárdenas *et al.* 2012) suggested that these structures are associated with either Sevier or Laramide orogenic events that occurred in the United States. Following Fitz-Díaz *et al.* (2018), the kinematics, chronology and deformation style of thick-skinned structures of the Mexican Orogen may be correlated with those belonging to the Laramide structures of the United States. Most previous geochronological studies about the timing of the shortening across the Mexican Orogen were performed in the Sierra Madre Oriental physiographic province (Gray *et al.* 2001; Fitz-Díaz *et al.* 2014; Garduño-Martínez *et al.* 2015; Martini *et al.* 2016; Guerrero-Paz *et al.* 2020). The spatial and temporal distribution of foredeep deposits suggests that the shortening migrated from west to east in the Sierra Madre Oriental during Late Cretaceous to Eocene times (e.g. Martini *et al.* 2016; Guerrero-Paz *et al.* 2020). Furthermore, this progressive and episodic eastward migration of the deformation was also proposed by

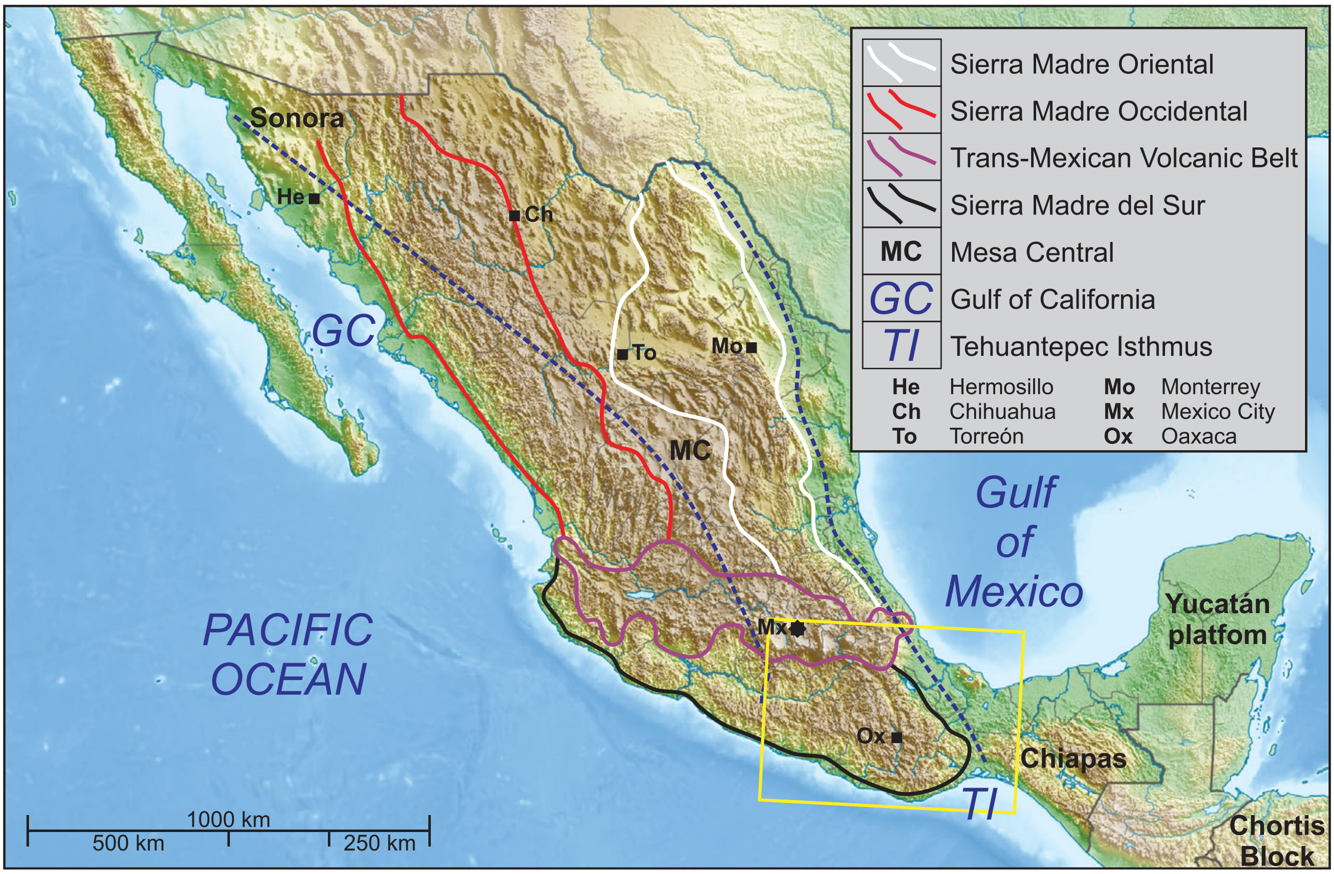


**Fig. 1.** (Colour online) Topographic map showing the main physiographic provinces of Mexico (modified after Fitz-Díaz *et al.* 2018). Dashed lines display the approximate distribution of the Mexican Orogen structures. The yellow rectangle approximately corresponds to the geological map depicted in Figure 2.

detailed structural analyses and geochronological studies carried out by Fitz-Díaz *et al.* (2012, 2014).

In southern Mexico, the Cretaceous–Cenozoic major lithological units and structures of the Sierra Madre del Sur are well known (e.g. Nieto-Samaniego *et al.* 2006). The Laramide *sensu lato* is considered the main cause of the contractile structures within the Sierra Madre del Sur; however, details about the migration, kinematics and intensity of deformation are poorly understood. Nieto-Samaniego *et al.* (2006) compiled published structural data and performed a detailed field-based study, analysing the geometry, kinematics and chronology of the main structures of southern Mexico. These authors proposed that the deformation migrated in the Sierra Madre del Sur from west to east between Maastrichtian and middle Eocene times and also recommended that more geochronological (thermochronological) data would be needed to establish the migration paths. Low-temperature thermochronometric techniques (i.e. He dating and fission-track analysis) have been applied sparsely to elucidating the timing of exhumation periods in the Sierra Madre del Sur (Ducea *et al.* 2004; Abdullin *et al.* 2021; Ramírez-Calderón *et al.* 2021). For example, Abdullin *et al.* (2021) reported apatite fission-track (AFT) data from the northern–central Grenvillian Oaxacan Complex and identified two Mesozoic cooling periods that were interpreted as resulting from exhumation: a Middle Triassic to Middle Jurassic cooling event that is probably linked to the break-up of Pangaea, and a younger one related to an exhumation episode during Early Cretaceous time that is coeval with the final stages of rifting of the Gulf of Mexico. Ramírez-Calderón *et al.* (2021) also detected Triassic-aged cooling signals from the Pennsylvanian–Cisuralian Totoltepec pluton, northeastern Acatlán Complex. However, there have been no detailed thermochronological studies performed to reconstruct the exhumation histories for the Late Cretaceous and Palaeogene period. In this work, we report the AFT results obtained from three different sectors of the Sierra Madre del Sur, which were obtained by laser ablation inductively coupled plasma mass spectrometry (LA-ICP-MS) for *in situ* quantification of $^{238}$U (Hasebe *et al.* 2004; Donelick *et al.* 2005; Vermeesch, 2017). The main objective of our study is the timing of the exhumation that took place in the Sierra Madre del Sur physiographic province during the Mexican Orogeny (or Laramide *sensu lato*). The results obtained during this work from three distinct study areas provide new insights into the deformation and exhumation history of the Sierra Madre del Sur during approximately Campanian–middle Eocene time.

## 2. Geological overview

The geological history of Mexico during the Mesozoic–Cenozoic period preserves a polyphase geodynamic evolution, and some significant tectonic events that occurred during those times may be described briefly as follows. During the Mesozoic period, the continental extensional tectonics was controlled by two important geodynamic processes: the subduction of the Farallon Plate beneath the western margin of North America and the rupture of Pangaea during Late Triassic–Middle Jurassic time (e.g. Martini & Ortega-Gutiérrez, 2018; Parolari *et al.* 2022). Martini

https://doi.org/10.1017/S0016756822000929 Published online by Cambridge University Press

*et al.* (2014) and Palacios-García & Martini (2014) suggested that the Late Jurassic to Early Cretaceous back-arc spreading of the Arperos Basin separated the Guerrero terrane from the Mexican mainland. After the accretion of the Guerrero composite terrane with the continental interior of Mexico, the Cretaceous sedimentation was dominantly calcareous (Fitz-Díaz *et al.* 2008). The Laramide *sensu lato* deformation event occurred after the accretion of the Guerrero terrane, and the shortening was active between Late Cretaceous and Eocene times (Nieto-Samaniego *et al.* 2006). It has been documented that the beginning and ending of the shortening deformation were diachronic (e.g. Cuéllar-Cárdenas *et al.* 2012; Martini *et al.* 2016; Fitz-Díaz *et al.* 2018).

The Sierra Madre del Sur, the principal object of this study, is located in southern Mexico and represents a large physiographic province composed of distinct crustal blocks with different lithologies bounded by major structures (Ortega-Gutiérrez *et al.* 2018). The crystalline basements of these blocks constitute outcrops of the lower and middle crust. According to the terrane division model of Sedlock *et al.* (1993), this physiographic province encompasses the Nahuatl, Mixteco, Zapoteco, Cuicateco, Chatino and Maya tectonostratigraphic terranes (Fig. 2). It is notable that most of the geological structures and the styles of deformation seem unrelated to terrane divisions (e.g. Nieto-Samaniego *et al.* 2006). In this study, we report the AFT results obtained from three study areas, presented here as three different sectors (Fig. 3). The geological settings for the studied sectors are described below.

### 2.a. Geology of the western sector

The western sector forms part of the Mixteco terrane (Figs 2, 3). This terrane is bounded by the Papalutla fault that separates the Mixteco terrane from the Nahuatl terrane, by the dextral-transpressional Caltepec fault zone to the east, which separates the Acatlán Complex from the Oaxacan Complex, as well as by the Chacalapa–La Venta fault system on the southern side (Fig. 2). The basement of the Mixteco terrane is represented by polymetamorphic rocks of the Palaeozoic Acatlán Complex. This metamorphic complex was originally divided into two tectonic assemblages: the structurally lower Petlalcingo subgroup and the upper Acateco subgroup (Ortega-Gutiérrez, 1978), both of which are components of a deformed thrust nappe overlain by upper Palaeozoic, low-grade metamorphic rocks. The geological record of this basement has undergone considerable revision in recent years owing to the improvement and enrichment of the geochronological, isotopic and palaeontological database (Keppie *et al.* 2008, 2018 and references therein). The Acateco subgroup includes the Piaxtla Suite and the Esperanza Granitoids, which underwent high-pressure metamorphism (e.g. Vega-Granillo *et al.* 2007). For the AFT analysis, we focused on the Esperanza Granitoids, which have been described as a sequence of metamorphosed and strongly deformed intrusive bodies such as granite and pegmatite (Ortega-Gutiérrez, 1978; Ortega-Gutiérrez *et al.* 1999; S. L. Florez-Amaya, unpub. M.Sc. thesis, Univ. Nacional Autónoma de México, 2021). According to J. Ramírez-Espinosa (unpub. Ph.D. thesis, Univ. Arizona, 2001) and M. Reyes-Salas (unpub. Ph. D. thesis, Univ. Autónoma del Estado de Morelos, 2003), the protolith for this unit is a peraluminous S-type granitic rock. The emplacement ages of the Esperanza Granitoids vary from ~485 Ma to ~440 Ma (Ortega-Gutiérrez *et al.* 1999; Talavera-Mendoza *et al.* 2005; Vega-Granillo *et al.* 2007; S. L. Florez-Amaya, unpub. M.Sc. thesis, Univ. Nacional Autónoma de México, 2021). Although some authors, for example, Vega-Granillo *et al.* (2007), have argued for a Silurian high-pressure metamorphism event recorded by mafic intrusions associated with the Esperanza Granitoids unit, presently available direct dating of the eclogite- and blueschist-facies metamorphism has yielded Mississippian dates, more precisely, at 353 ± 2 Ma (Estrada-Carmona *et al.* 2016; S. L. Florez-Amaya, unpub. M.Sc. thesis, Univ. Nacional Autónoma de México, 2021).

### 2.b. Geology of the central sector

The central sector is located within an area between the Mixteco and Zapoteco tectonostratigraphic terranes (Figs 2, 3). For the AFT analysis in this sector, most samples were collected from the Matzitzi Formation. This unit unconformably overlies Palaeozoic and Proterozoic rocks belonging to the Acatlán and Oaxacan complexes (e.g. Centeno-García *et al.* 2009; Bedoya *et al.* 2021). The Oaxacan Complex is mainly composed of Proterozoic, granulite-facies, mafic to felsic gneisses as well as numerous pegmatitic intrusions (Shchepetilnikova *et al.* 2015). The boundary between the Oaxacan and the Acatlán complexes is a NNE-trending dextral transpressive shear zone, i.e. the Caltepec fault zone (Elías-Herrera *et al.* 2005). The ~270 Ma age Cozahuico pluton (Fig. 3) is exposed along the Caltepec fault and is interpreted as a syntectonic intrusion dating the collision between the Oaxacan and Acatlán complexes (Elías-Herrera *et al.* 2005). The Matzitzi Formation was first described by Aguilera (1896), and then defined by Calderón-García (1956) as a succession composed of sandstone, dark shale, conglomerate and coal containing a diverse fossil flora. Centeno-García *et al.* (2009) recognized in the Matzitzi Formation the typical facies associations that characterize modern anastomosing fluvial systems. The age of the Matzitzi Formation has been an object of debate for decades (for example, see details in Bedoya *et al.* 2021; Martini *et al.* 2022). Based on stratigraphic correlations, Aguilera (1896) and Calderón-García (1956) first proposed a Triassic and Jurassic age, respectively. Later, Silva (1970) reported the occurrence of Pennsylvanian fossil plants in the Matzitzi Formation. After a careful re-evaluation of the flora association studied by Weber (1997), Flores-Barragán *et al.* (2019) assigned a late Permian age to the Matzitzi Formation. This depositional age was confirmed by recent geochronological studies performed by Martini *et al.* (2022).

### 2.c. Geology of the eastern sector

The eastern sector is located within the Cuicateco terrane (Fig. 2). In this study area, we sampled the Chivillas Formation for analysis by the AFT method. The age of the crystalline basement upon which the Chivillas Formation was deposited is still unconstrained. This formation is in fault contact with the Oaxacan Complex (Fig. 3). This contact had multiple reactivations, the youngest as a Cenozoic normal fault (i.e. the Oaxaca fault; Fig. 2). The basin-fill covers the contact between the Cuicateco terrane and the Oaxacan Complex. Most rocks from the Cuicateco terrane belong to the Sierra de Juárez mylonitic belt, composed of mylonitized gneisses and volcano-sedimentary rocks as well as serpentinites (Delgado-Argote, 1988). The Sierra de Juárez mylonitic belt was formed in a dextral strike-slip fault (Alaniz-Álvarez *et al.* 1994). The radiometric ages from this belt range between 192 ± 1 Ma (i.e. the protolith age of a syntectonic metagranite; Espejo-Bautista *et al.* 2022) and 169 ± 2 Ma (muscovite $^{40}Ar$–$^{39}Ar$ age; Alaniz-Álvarez *et al.* 1996). The serpentinitic bodies yielded hornblende $^{40}Ar$–$^{39}Ar$ cooling ages of 138 ± 8, 132 ± 4 and 123 ± 7 Ma (Delgado-Argote *et al.* 1992). The Sierra de

https://doi.org/10.1017/S0016756822000929 Published online by Cambridge University Press

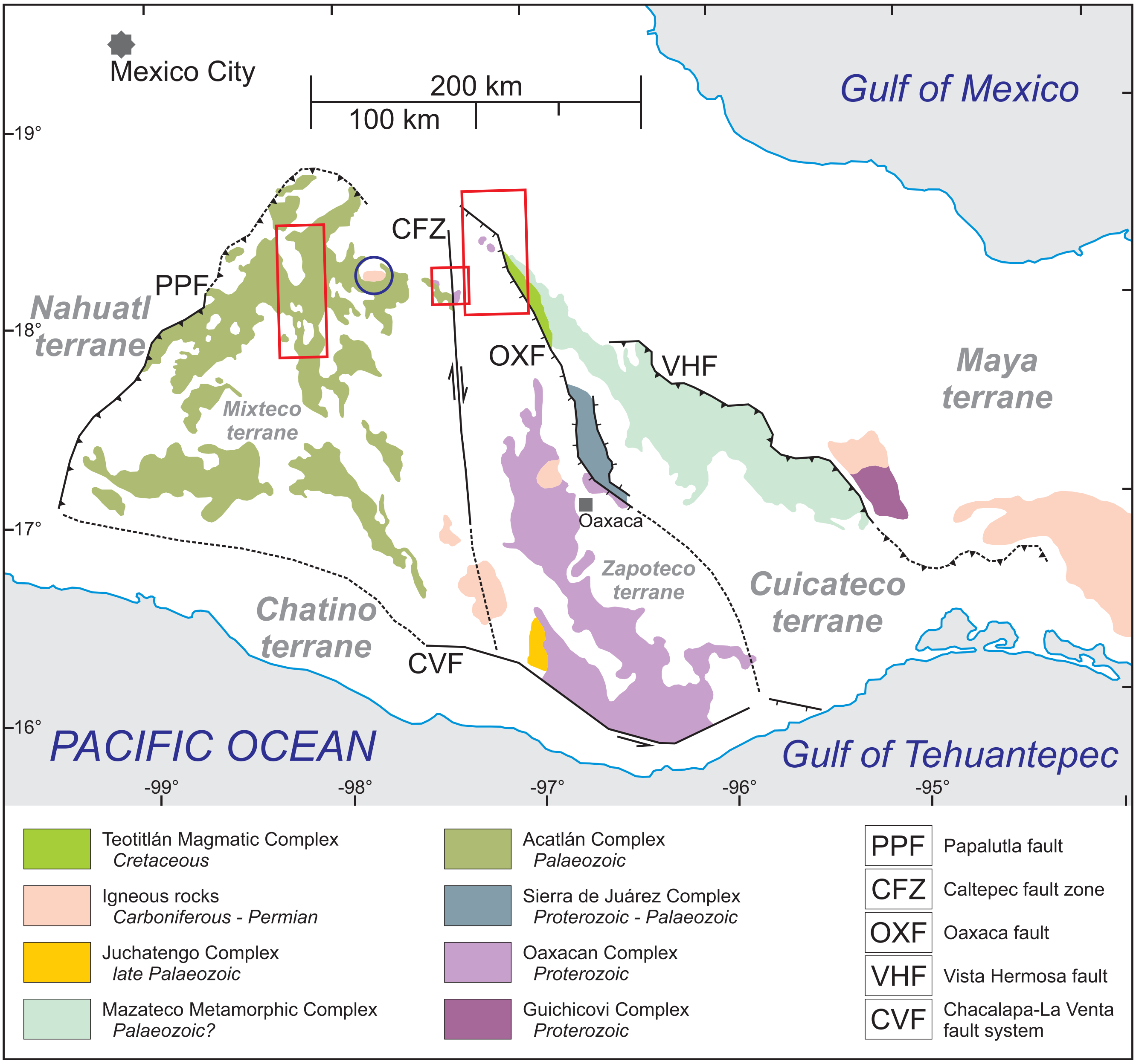


**Fig. 2.** (Colour online) Geological map showing basement lithologies and tectonostratigraphic terranes of southern Mexico (according to Ortega-Gutiérrez *et al.* 2018; Espejo-Bautista *et al.* 2022). Red rectangular regions represent the studied sectors where apatite fission-track results were obtained during this study (see also Fig. 3 for details). Blue circle is the area studied by M. G. Ramírez-Calderón (unpub. M.Sc. thesis, Univ. Nacional Autónoma de México, 2018).

Juárez mylonitic belt is thrust over the oldest rocks of the Cuicateco terrane (i.e. the Mazateco Complex), made up of schist and amphibolite of probably Palaeozoic age (Mendoza-Rosales *et al.* 2010). The Cuicateco terrane also contains thick limestone units. The mylonitic rocks are thrust over the limestone units. To the south, the Mazateco Complex is thrust over Upper Triassic(?) to Jurassic (e.g. Pérez-Gutiérrez *et al.* 2009) red beds from the Todos Santos Formation. The Chivillas Formation consists of a quite thick succession of pillow lavas and basaltic lava flows, interbedded with turbidites and is overlain depositionally by limestone. Mendoza-Rosales *et al.* (2010) interpreted the upper contact of the Chivillas Formation as transitional, based on the gradational change from siliciclastic turbidites to calcareous turbidites belonging to the Miahuatepec Formation. Based on detrital zircon U–Pb dating, a Barremian stratigraphic age was preliminarily proposed for the Chivillas Formation (Mendoza-Rosales *et al.* 2010). The deformation history of the Cuicateco terrane is very complex, and some authors have detected three to five different deformation episodes (e.g. Alaniz-Álvarez *et al.* 1996; E. Ángeles-Moreno, unpub. M.Sc. thesis, Univ. Nacional Autónoma de México, 2006; Mendoza-Rosales *et al.* 2010).

## 3. Samples and methods

To detect Late Cretaceous and Cenozoic cooling ages, we sampled those areas that are close to key regional structures (Figs 2, 3), as was recommended by Abdullin *et al.* (2021). A total of four augen gneiss samples were collected from the Esperanza Granitoids in the

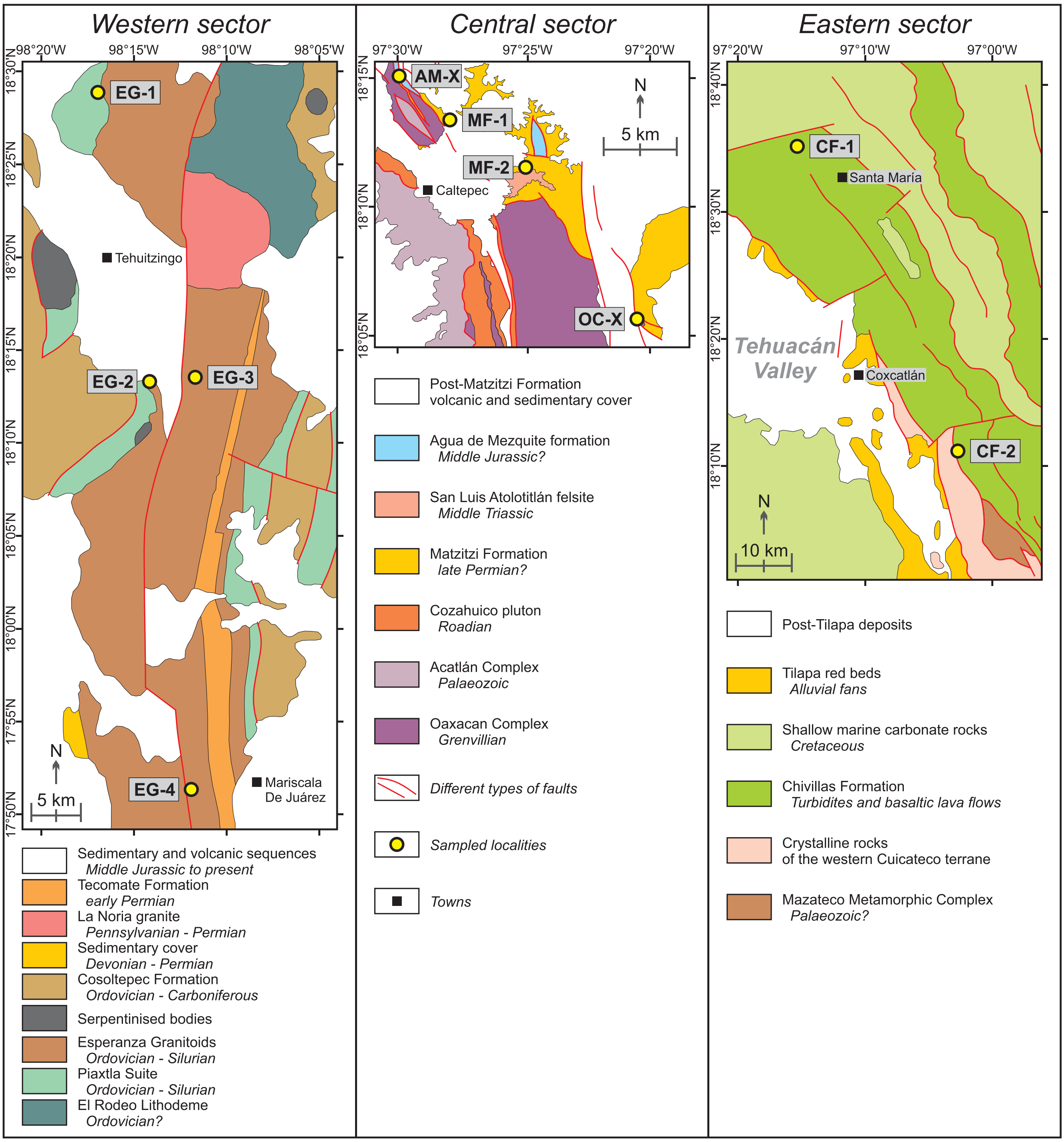


**Fig. 3.** (Colour online) Simplified geological maps of the western, central and eastern sectors displaying the sampled points (western sector – data according to Ortega-Gutiérrez *et al.* 2018; central sector – data according to Bedoya *et al.* 2021; Martini *et al.* 2022; eastern sector – data from R. E. Milián de la Cruz, unpub. M.Sc. thesis, Univ. Nacional Autónoma de México, 2019).

western sector (EG-1, EG-2, EG-3 and EG-4; Fig. 3). In the central study area, we primarily focused on the late Permian Matzitzi Formation (sandstone samples MF-1 and MF-2; Fig. 3). In this area, additionally, one sample (AM-X; sandstone) from the Agua de Mezquite formation (a Middle Jurassic? clastic unit; Bedoya *et al.* 2021) and another one from the Grenvillian Oaxacan Complex (OC-X; granulite gneiss) were also obtained for the AFT thermochronology. Two sandstone samples, CF-1 and CF-2, were collected from the Barremian(?) Chivillas Formation in the easternmost sector (Fig. 3).

Heavy minerals from the collected samples were concentrated using conventional mineral separation techniques such as crushing, sieving, Wilfley table, Frantz separator, and heavy liquids (we used bromoform and sodium polytungstate). Approximately 500 apatite grains, extracted from each concentrate sample under a dissecting microscope, were mounted with EpoFix (Struers) in a 2.5 cm diameter

**Table 1.** LA-ICP-MS-based apatite fission-track results obtained from three different study areas across the Sierra Madre del Sur, southern Mexico

| Sample | Geographic coordinates | Ngr | Central age (Ma) | *D* (%) | $P(\chi^2)$ | MTL with *SD* (µm) | Ntr | Average Cl with *SD* (wt %) |
|---|---|---|---|---|---|---|---|---|
| ***Western sector*** | | | | | | | | |
| EG-1 | 18° 28′ 53″ N/98° 17′ 36″ W | 8 | 57 ± 3 | 0 | 0.48 | – | – | 0.670 ± 0.208 |
| EG-2 | 18° 13′ 37″ N/98° 14′ 43″ W | 45 | 69 ± 1 | 3 | 0.32 | 12.81 ± 1.48 | 153 | 0.591 ± 0.295 |
| EG-3 | 18° 13′ 36″ N/98° 11′ 42″ W | 17 | 69 ± 3 | 0 | 0.25 | – | – | 0.701 ± 0.137 |
| EG-4 | 17° 51′ 15″ N/98° 11′ 37″ W | 22 | 60 ± 2 | 8 | 0.17 | 13.07 ± 1.35 | 55 | 0.515 ± 0.136 |
| ***Central sector*** | | | | | | | | |
| AM-X | 18° 15′ 09″ N/97° 29′ 42″ W | 40 | 60 ± 2 | 8 | 0.08 | 13.15 ± 1.38 | 69 | 0.706 ± 0.418 |
| MF-1 | 18° 13′ 18″ N/97° 27′ 45″ W | 78 | 59 ± 1 | 0 | 0.51 | – | – | 0.846 ± 0.342 |
| MF-2 | 18° 11′ 36″ N/97° 25′ 07″ W | 31 | 61 ± 2 | 7 | 0.13 | 13.16 ± 1.10 | 64 | 0.777 ± 0.303 |
| OC-X | 18° 05′ 31″ N/97° 20′ 21″ W | 26 | 61 ± 3 | 0 | 1.00 | – | – | 0.566 ± 0.148 |
| ***Eastern sector*** | | | | | | | | |
| CF-1 | 18° 35′ 10″ N/97° 15′ 19″ W | 84 | 40 ± 1 | 14 | 0.19 | 13.30 ± 1.35 | 44 | 0.437 ± 0.232 |
| CF-2 | 18° 11′ 08″ N/97° 02′ 41″ W | 72 | 41 ± 1 | 0 | 0.60 | 13.08 ± 1.27 | 65 | 0.656 ± 0.114 |

*Note:* Ngr is the number of grains dated. The central ages (i.e. weighted mean ages) were obtained using RadialPlotter (Vermeesch, 2009). *D* and $P(\chi^2)$ are the dispersion of ages and the chi-squared probability test, respectively. MTL represents the mean track length. Ntr is the number of confined track lengths tested (only track-in-track-type horizontally confined tracks were measured; e.g. please see details in Donelick *et al.* 2005). Cl is the chlorine content determined with LA-ICP-MS. The types of samples (i.e. lithologies and ages) can be consulted in the main text.

plastic ring (i.e. most crystals were mounted with their surfaces parallel to the *c*-axis). Mounted crystals were polished to expose their internal surfaces (i.e. for $4\pi$ geometry), and then were etched in 5.5M $HNO_3$ at 21 °C for 20 s to reveal spontaneous fission tracks (e.g. see Donelick *et al.* 2005). Fission-track counting and track length measurements were performed using a Zeiss AxioScope.A1 microscope upgraded with a digital camera, image processing software and dry objectives. LA-ICP-MS-based single-spot analyses, using a laser beam spot diameter of ~60 µm, were performed exactly within the same counting areas observed previously to obtain the spontaneous track densities (Abdullin *et al.* 2016; Vermeesch, 2017). Polished and etched sections of Durango F-apatite parallel to the crystallographic *c*-axis were also analysed during the same sessions of track counting and LA-ICP-MS analysis. This fluorapatite, with a standard age of 31.4 ± 0.5 Ma (e.g. Solé & Pi, 2005; Abdullin *et al.* 2014), was used for $\zeta$-equivalent calibration (Hasebe *et al.* 2004; Donelick *et al.* 2005; Vermeesch, 2017, 2018) as well as to determine chlorine levels in unknown apatite grains (i.e. Durango, with an average Cl of 0.43 ± 0.04 wt %, was used as a primary standard for Cl measurements; Chew *et al.* 2014). Raw data were reduced using Iolite 3.4 (Paton *et al.* 2011). The results for measured isotopes using NIST612 (Pearce *et al.* 1997) were normalized using $^{43}$Ca as an internal standard and taking an average CaO of 55 % for all apatite grains analysed. Single-grain AFT ages and 1σ-errors were calculated with IsoplotR (Vermeesch, 2018). The central (i.e. weighted mean) ages were obtained with RadialPlotter (Vermeesch, 2009). LA-ICP-MS AFT analysis was carried out at Laboratorio de Estudios Isotópicos (LEI), Centro de Geociencias, Campus Juriquilla, Universidad Nacional Autónoma de México. The LA-ICP-MS protocol (including laser ablation and ICP-MS operating conditions, data acquisition parameters, scheme of microsampling, measured isotopes, etc.) used routinely at LEI for apatite is described in detail by Ortega-Obregón *et al.* (2019) and Ramírez-Calderón *et al.* (2021).

## 4. Apatite fission-track results

The AFT results obtained from all the analysed rock samples are summarized in Table 1 and Figure 4, while detailed information on our fission-track and LA-ICP-MS experiments (number of tracks counted, confined track length measurements, $^{238}$U and Cl concentrations, single-grain ages with $1\sigma$-errors, analytical uncertainties, etc.) are given in the online Supplementary Material. The AFT-based time–temperature (*t*–*T*) histories were reconstructed for six samples (EG-2, EG-4, AM-X, MF-2, CF-1 and CF-2) using HeFTy 1.9.3 (Ketcham, 2005) with inverse Monte Carlo modelling and based on the multicomponent annealing model of Ketcham *et al.* (2007). The 'best-fit' cooling curves were obtained testing 200 'good' thermal history scenarios. Most apatite grains analysed during this study are F-apatite, with average Cl contents of less than 0.9 wt % (Table 1). The closure temperature for the AFT system in most common apatite specimens, i.e. in F-apatite, generally varies between ~120 and 90 °C depending on the cooling rates (Donelick *et al.* 2005). For fission tracks in F-apatite, the temperature span of ~60–110 °C is referred to as the partial annealing zone (Gleadow *et al.* 1986). Boxes limiting possible solutions to the *t*–*T* models (Fig. 5) were added based on known and reasonable geological constraints (Abdullin *et al.* 2016, 2018, 2021; A. M. Bedoya-Mejía, unpub. M.Sc. thesis, Univ. Nacional Autónoma de México, 2018; M. G. Ramírez-Calderón, unpub. M.Sc. thesis, Univ. Nacional Autónoma de México, 2018; R. E. Milián de la Cruz, unpub. M.Sc. thesis, Univ. Nacional Autónoma de México, 2019; S. L. Florez-Amaya, unpub. M.Sc. thesis, Univ. Nacional Autónoma de México, 2021).

### 4.a. AFT results from the western sector

The central AFT ages, obtained for four gneiss samples from the Esperanza Granitoids (Acatlán Complex), range from 69 ± 3 ($1\sigma$) Ma (sample EG-3) to 57 ± 3 ($1\sigma$) Ma (for EG-1) (Table 1; Fig. 4). All the dated samples passed the chi-squared probability test with $P(\chi^2)$ higher than 0.05 (Fig. 4), indicating that these apatite groups represent a single cooling event. Track length measurements were performed for two samples, EG-2 and EG-4, which have mean track length (MTL) values of 12.81 ± 1.48 (*SD*) µm and 13.07 ± 1.35 (*SD*) µm, respectively (Table 1). The results of the *t*–*T* modelling performed for samples EG-2 and EG-4 are given in Figure 5.

https://doi.org/10.1017/S0016756822000929 Published online by Cambridge University Press

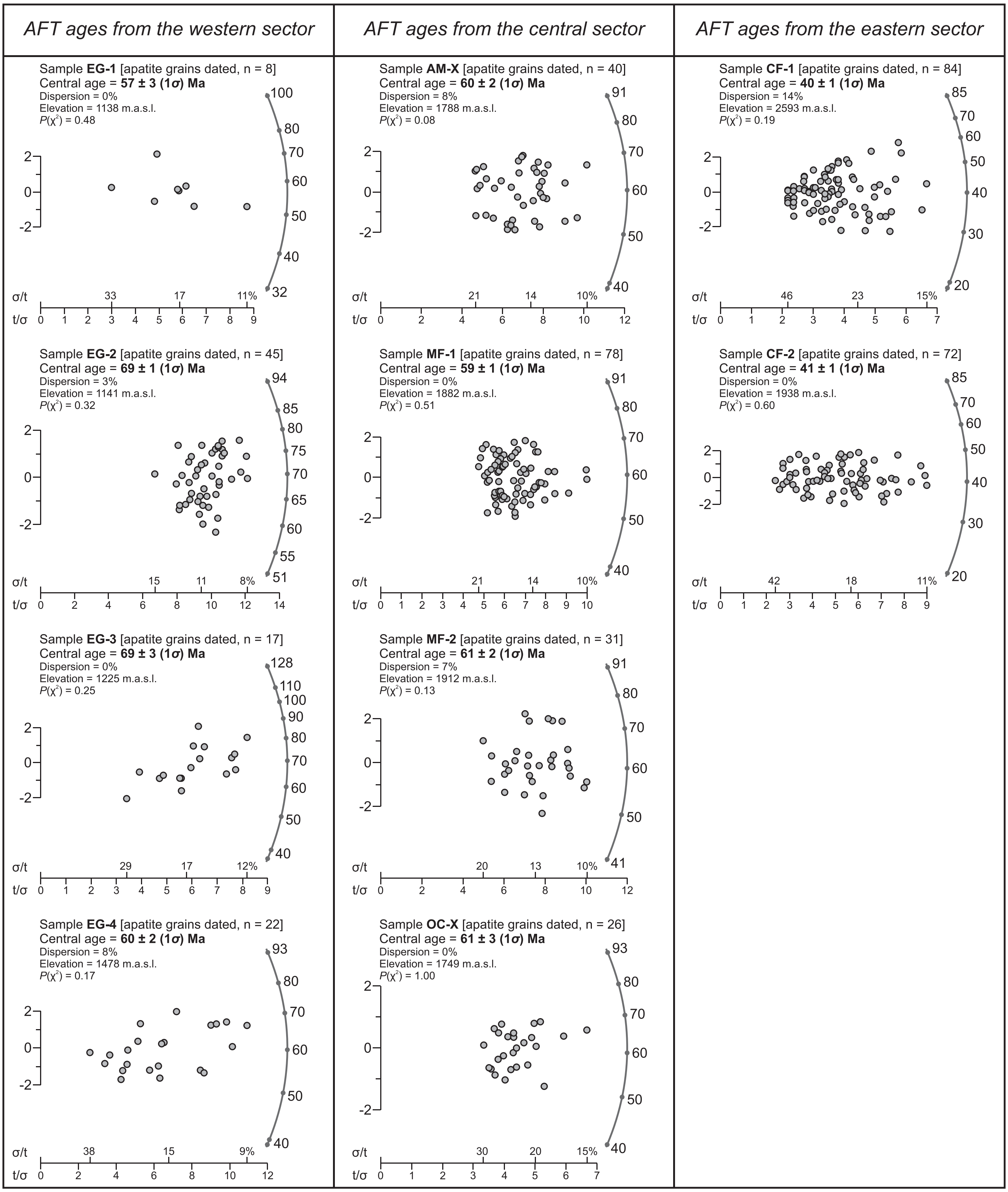


**Fig. 4.** Apatite fission-track (AFT) results obtained from the three studied sectors.

## 4.b. AFT results from the central sector

As shown in Figure 4, all the four samples yielded similar central AFT ages (i.e. ~60 Ma; see also Table 1) of 60 ± 2 (1$\sigma$) Ma for sample AM-X, 59 ± 1 (1$\sigma$) Ma for MF-1, 61 ± 2 (1$\sigma$) Ma in MF-2 and 61 ± 3 (1$\sigma$) Ma for the Grenvillian sample OC-X. These cooling ages are significantly younger than the stratigraphic ages of the Matzitzi Formation (late Permian; Martini *et al.* 2022) and the

https://doi.org/10.1017/S0016756822000929 Published online by Cambridge University Press

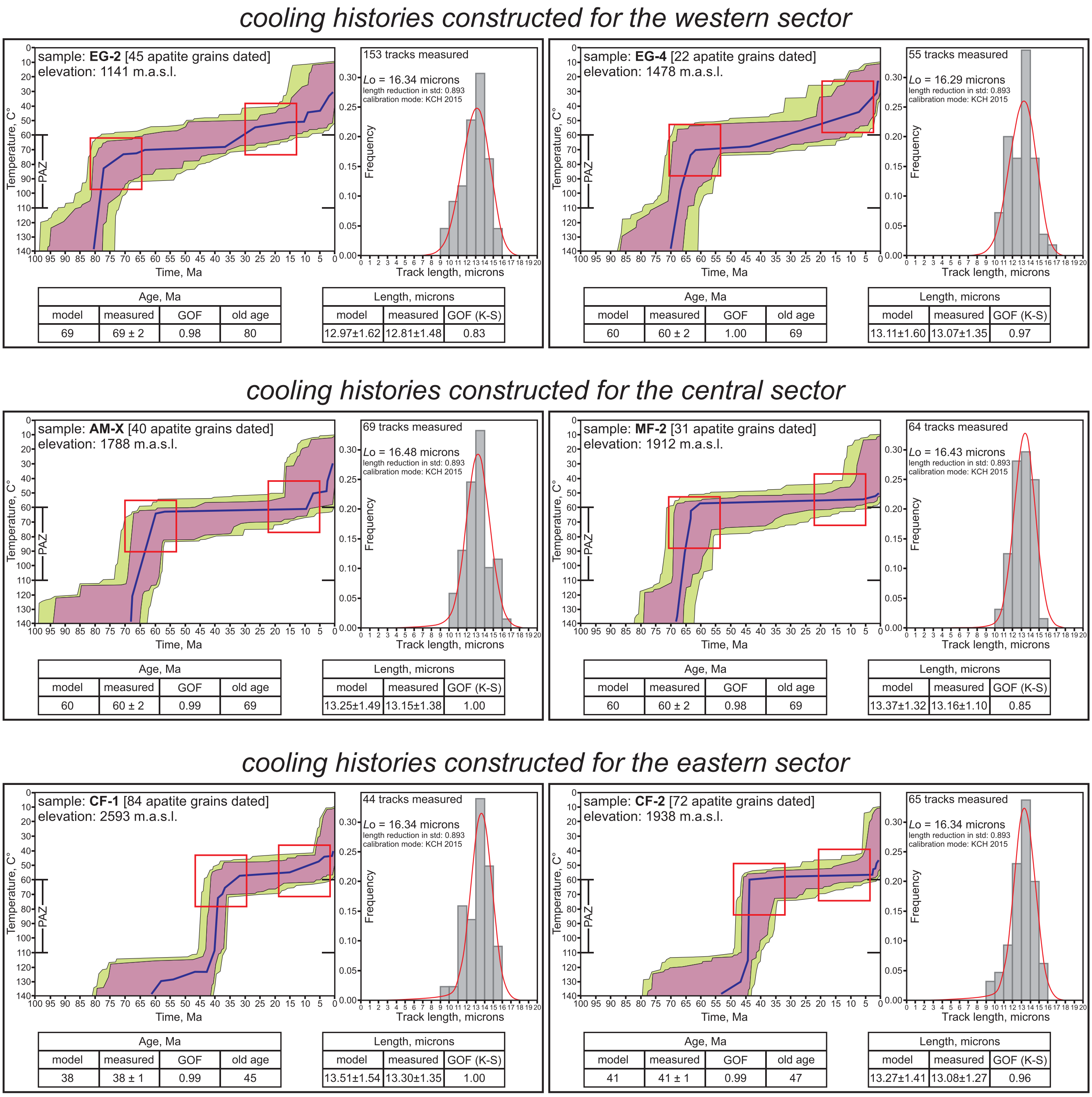


**Fig. 5.** (Colour online) Apatite fission-track (AFT)-based time–temperature modelling. PAZ – partial annealing zone for the AFT chronometry. Purple areas in the models represent 'good' thermal history scenarios, while green areas represent 'acceptable' paths. Solid lines represent the 'best-fit' cooling histories. GOF – goodness-of-fit between the measured and the model ages. GOF (K-S) – goodness-of-fit between the measured and the model fission-track lengths. K-S – Kolmogorov–Smirnov test.

Agua de Mezquite unit (Middle Jurassic?; Bedoya *et al.* 2021). This implies that detrital apatite grains from the studied sandstone samples AM-X, MF-1 and MF-2 were reset totally for the AFT system after their deposition, certainly due to burial-related heating of these clastic units during diagenesis. All these samples passed the chi-squared probability test with $P(\chi^2)$ values of 0.08 for sample AM-X, 0.51 for MF-1, 0.13 for MF-2 and 1.00 for sample OC-X (Fig. 4). Track length measurements were performed for two samples, AM-X and MF-2, which yielded MTLs of 13.15 ± 1.38 (*SD*) and 13.16 ± 1.10 (*SD*) μm, respectively (Table 1). This implies that these detrital apatite populations belong to a single monotonic cooling event. The cooling histories obtained from samples AM-X and MF-2 are displayed in Figure 5.

### 4.c. AFT results from the eastern sector

Two clastic samples from the Barremian Chivillas Formation (Mendoza-Rosales *et al.* 2010), CF-1 and CF-2, were analysed using the AFT technique. These samples yielded identical central ages of 40 ± 1 (1$\sigma$) Ma (sample CF-1) and 41 ± 1 (1$\sigma$) Ma (CF-2). Both samples passed the chi-squared probability test with $P(\chi^2)$ higher than 0.05 (Table 1; Fig. 4). These sandstone samples display

https://doi.org/10.1017/S0016756822000929 Published online by Cambridge University Press

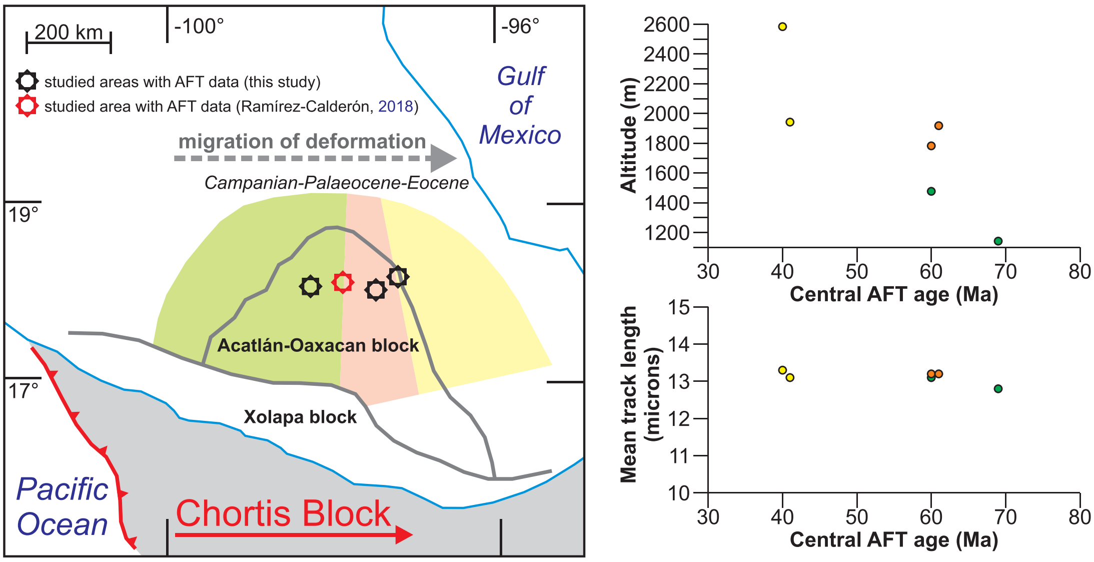


**Fig. 6.** (Colour online) Simplified reconstruction of the tectonic evolution of southern Mexico during Campanian–Eocene time (modified from Nieto-Samaniego *et al.* 2006).

AFT ages that are younger than the depositional age of the Chivillas Formation. CF-1 and CF-2 have MTL values of 13.3 ± 1.35 (*SD*) μm and 13.08 ± 1.27 (*SD*) μm, respectively (Table 1). The AFT results obtained from the Chivillas Formation indicate that both samples cooled rapidly through the partial annealing zone of ~60–110/120 °C. HeFTy-derived cooling paths constructed for the Chivillas Formation are presented in Figure 5.

## 5. Discussion and concluding remarks

The development of extensive Cretaceous platforms with deposition of thick carbonate successions along the rim of the Gulf of Mexico (Wilson & Ward, 1993; Padilla y Sánchez, 2007) was enough to reset apatite grains for the fission-track chronometry in the rocks, particularly in clastic ones (i.e. in samples of the Agua de Mezquite, Matzitzi and Chivillas formations), owing to burial-related heating during diagenesis. In these areas, the thermochronometric results should represent the cooling histories controlled by relatively young exhumation processes (i.e. post-platform ages). The AFT ages decrease from west to east (i.e. from the Mixteco terrane through Zapoteco to the Cuicateco terrane; Fig. 2): from ~70 to 60 Ma in the western part through ~60 Ma in the central part to ~40 Ma in the eastern sector (Fig. 4), a time span that is interpreted as a period of cooling of the Sierra Madre del Sur due to the exhumation and erosion between Late Cretaceous and middle Eocene times. This exhumation period was also observed in Chiapas, southeastern Mexico (Fig. 1), which could be interpreted as the southernmost continuation of the Late Cretaceous–Eocene orogenic system in Mexico (Meneses-Rocha, 2001; Padilla y Sánchez, 2007; Abdullin *et al.* 2016, 2018). According to Martini *et al.* (2016), the shortening of the westernmost part (i.e. the Sierra de los Cuarzos area) of the Sierra Madre Oriental started in Campanian time. Radiometric data compiled in Guerrero-Paz *et al.* (2020) for the Sierra Madre Oriental as well as our AFT data obtained from the Sierra Madre del Sur support that the deformation initiated in Campanian time, because K–Ar and $^{40}Ar$–$^{39}Ar$ dates of authigenic illite determined in shear zones and folds from the Sierra Madre Oriental (Fitz-Díaz *et al.* 2014; Garduño-Martínez *et al.* 2015; Martini *et al.* 2016), along with the AFT ages obtained in the Sierra Madre del Sur (this study), are younger than 85 Ma. Further, M. G. Ramírez-Calderón (unpub. M.Sc. thesis, Univ. Nacional Autónoma de México, 2018) reported young AFT peaks at 88 ± 8, 78 ± 5 and 64 ± 6 Ma from the Totoltepec pluton, Acatlán Complex (circle-shaped study area in Fig. 2), cooling ages which lie roughly in the Santonian–Maastrichtian period. These AFT ages were tentatively interpreted by M. G. Ramírez-Calderón (unpub. M.Sc. thesis, Univ. Nacional Autónoma de México, 2018) as belonging to the Mexican Orogen.

Thermal history models indicate that the exhumation migrated across the Sierra Madre del Sur from west to east between Late Cretaceous and middle Eocene times (Fig. 5), a tectonic activity that is coeval with the Laramide *sensu lato* (Mexican Orogen) as was previously suggested by Nieto-Samaniego *et al.* (2006). Samples EG-2 and EG-4, obtained from the western area, detected an exhumation period for a time interval of ~80–60 Ma (Campanian to Paleocene) with a low cooling rate of ~4 °C $Ma^{-1}$. In contrast, in the central and eastern sectors, the analysed samples yielded younger cooling episodes of ~70–60 Ma (Maastrichtian to Paleocene) and ~45–35 Ma (i.e. middle Eocene) with moderate and elevated cooling rates of ~12 °C $Ma^{-1}$ and ~17 °C $Ma^{-1}$, respectively (Fig. 5). The AFT cooling ages become younger from west to east across the Sierra Madre del Sur, whereas the cooling rates become higher in the same direction. Our AFT results (in particular, the cooling rates; Fig. 5), thus, confirm that the deformation and associated exhumation migrated from west to east during Campanian–middle Eocene time. The AFT ages obtained during this study were mainly interpreted as belonging to the Laramide *sensu lato* shortening event. However, ~45–35 Ma cooling ages with high cooling rates (Fig. 5) in the easternmost sector (Cuicateco terrane) are most likely related to an early extensional phase that initiated approximately during middle Eocene time (e.g. Dávalos-Álvarez *et al.* 2007), shortly after the end of the Laramide *sensu lato*. This extensional event reactivated the Oaxaca fault in Eocene time as a normal fault producing the Tehuacán Valley with deposition of the Tilapa red beds (Fig. 3) and uplift and erosion of the Mazateca range (Nieto-Samaniego *et al.* 2006; Dávalos-Álvarez *et al.* 2007).

According to some authors, for example, Fitz-Díaz *et al.* (2018), active magmatism during the entire evolution of the Mexican Orogen implicates the subducted Farallon slab as a principal driver of crustal thickening. Besides, deformation–magmatic cycles coincide well with periods of westward acceleration of the North America Plate and further corroborate subduction as the main geodynamic driver for the Mexican orogenesis during Late Cretaceous–Eocene time (van der Meer *et al.* 2010; Fitz-Díaz *et al.* 2018). In southern Mexico, the convergence between circum-Pacific terranes (e.g. the Guerrero terrane and the Chortis Block) and mainland southern Mexico (Mixteco and Zapoteco) may have triggered thickening and orogenic metamorphism of the Mesozoic crust of the Xolapa Complex (i.e. part of the Chatino terrane; Fig. 2) (Maldonado *et al.* 2020). Therefore, the possible influence of movement of the Chortis Block on the development of the Sierra Madre del Sur cannot be ruled out (Nieto-Samaniego *et al.* 2006; Maldonado *et al.* 2020) (see simplified reconstruction in Fig. 6). Based on the available chronological dataset, it cannot be proposed that the Sierra Madre del Sur was formed by a single orogenic event or by multiple pulses during Late Cretaceous to Eocene times. To resolve this doubt, additional structural and detailed thermochronological data are required from further studies of distinct areas along the whole Mexican Orogen. Nevertheless, and this is the finding of our study, the cooling rates increased systematically in the Sierra Madre del Sur from west to east approximately between Campanian and middle Eocene times. Abdullin *et al.* (2021), based on AFT results obtained from the Oaxacan Complex, suggested that the major fault systems of the Sierra Madre del Sur including the Caltepec and the Oaxaca faults (Fig. 2) have remained episodically active since, at least, Middle Triassic time. In our view, the activity of these large fault systems played a key role in the formation of geological structures as well as in the exhumation of the Sierra Madre del Sur during the Campanian–middle Eocene Laramide *sensu lato*.

**Supplementary material.** For supplementary material accompanying this paper visit https://doi.org/10.1017/S0016756822000929

**Acknowledgements.** The authors are very grateful to Juan Tomás Vazquez Ramírez and Ofelia Pérez Arvizu (both from Centro de Geociencias, UNAM) for their help with sample preparation for AFT analysis. Sandra Lorena Florez-Amaya, Alejandra Bedoya-Mejía and Ricardo Enrique Milián de la Cruz thank CONACyT for scholarships. Roberto Maldonado acknowledges DGAPA UNAM for a postdoctoral fellowship. This research was supported by the PAPIIT DGAPA UNAM project IN101520, granted to Luigi Solari. The second author also thanks Mónica Ramírez-Calderón and Sandra Guerrero Moreno (both *fodongas* from PCT, UNAM) for early comments that helped to improve this work. Gilby Jepson, one anonymous reviewer, and the associate editors (Professor Olivier Lacombe and Professor Guido Meinhold) are acknowledged for their constructive suggestions that improved our manuscript significantly.

**Conflict of interest.** None.

## References

**Abdullin F, Solari L, Ortega-Obregón C and Solé J** (2018) New fission-track results from the northern Chiapas Massif area, SE Mexico: trying to reconstruct its complex thermo-tectonic history. *Revista Mexicana de Ciencias Geológicas* **35**, 79–92. doi: 10.22201/cgeo.20072902e.2018.1.523.

**Abdullin F, Solari L, Solé J and Ortega-Obregón C** (2021) Mesozoic exhumation history of the Grenvillian Oaxacan Complex, southern Mexico. *Terra Nova* **33**, 86–94. doi: 10.1111/ter.12493.

**Abdullin F, Solé J, Meneses-Rocha JDJ, Solari L, Shchepetilnikova V and Ortega-Obregón C** (2016) LA-ICP-MS-based apatite fission track dating of the Todos Santos Formation sandstones from the Sierra de Chiapas (SE Mexico) and its tectonic significance. *International Geology Review* **58**, 32–48. doi: 10.1080/00206814.2015.1055596.

**Abdullin F, Solé J and Solari L** (2014) Datación mediante trazas de fisión y análisis multielemental con LA-ICP-MS del fluorapatito de Cerra de Mercado (Durango, México). *Revista Mexicana de Ciencias Geológicas* **31**, 395–406.

**Aguilera JG** (ed.) (1896) *Bosquejo Geológico de México*. Boletin del Instituto Geológico de México **4–6**, 270 pp.

**Alaniz-Álvarez SA, Nieto-Samaniego AF and Ortega-Gutiérrez F** (1994) Structural evolution of the Sierra Juárez Mylonitic Complex, State of Oaxaca, Mexico. *Revista Mexicana de Ciencias Geológicas* **11**, 147–56.

**Alaniz-Álvarez SA, van der Heyden P, Nieto Samaniego AF and Ortega-Gutiérrez F** (1996) Radiometric and kinematic evidence for Middle Jurassic strike-slip faulting in southern Mexico related to the opening of the Gulf of Mexico. *Geology* **24**, 443–6. doi: 10.1130/0091-7613(1996)024<0443:RAKEFM>2.3.CO;2.

**Bedoya A, Anaya-Guarneros JA, Abdullin F, Martini M and Solari L** (2021) Provenance analysis of the Matzitzi and Agua de Mezquite formations, southern Mexico: different fluvial successions formed during late Paleozoic and post-Middle Jurassic time along the southernmost North America Pacific margin. *Journal of South American Earth Sciences* **105**, 102999. doi: 10.1016/j.jsames.2020.102999.

**Calderón-García A** (1956) Bosquejo geológico de la región de San Juan Raya, Puebla. In *XX Congreso Internacional, Libreto Guía, Excursión A-11: estratigrafía del Mesozoico y tectónica del sur del estado de Puebla; Presa de Valsequillo, Sifón de Huexotitlanapa y problemas hidrológicos de Puebla*, pp. 9–27. Universidad Nacional Autónoma de México.

**Campa MF and Coney PJ** (1983) Tectono-stratigraphic terranes and mineral resource distributions in Mexico. *Canadian Journal of Earth Sciences* **20**, 1040–51. doi: 10.1139/e83-094.

**Centeno-García E, Mendoza-Rosales CC and Silva-Romo G** (2009) Sedimentología de la Formación Matzitzi (Paleozoico superior) y significado de sus componentes volcánicos, región de Los Reyes Metzontla–San Luis Atolotitlán, Estado de Puebla. *Revista Mexicana de Ciencias Geológicas* **26**, 18–36.

**Cerca M, Ferrari L, López-Martínez M, Martiny B and Iriondo A** (2007) Late Cretaceous shortening and early Tertiary shearing in the central Sierra Madre del Sur, southern Mexico: insights into the evolution of the Caribbean–North American plate interaction. *Tectonics* **26**, TC3007. doi: 10.1029/2006TC001981.

**Chew DM, Donelick RA, Donelick MB, Kamber BS and Stock MJ** (2014) Apatite chlorine concentration measurements by LA-ICP-MS. *Geostandards and Geoanalytical Research* **38**, 23–35. doi: 10.1111/j.1751-908X.2013.00246.x.

**Cuéllar-Cárdenas MA, Nieto-Samaniego AF, Levresse G, Alaniz-Álvarez SA, Solari L, Ortega-Obregón C and López-Martínez M** (2012) Límites temporales de la deformación por acortamiento Laramide en el centro de México. *Revista Mexicana de Ciencias Geológicas* **29**, 179–203.

**Dávalos-Álvarez OG, Nieto-Samaniego AF, Alaniz-Álvarez SA, Martínez-Hernández E and Ramírez-Arriaga E** (2007) Estratigrafía cenozoica de la región de Tehuacán y su relación con el sector norte de la falla de Oaxaca. *Revista Mexicana de Ciencias Geológicas* **24**, 197–215.

**Delgado-Argote LA** (1988) Geología preliminar de la secuencia volcanosedimentaria y serpentinitas asociadas del Jurásico (?) del área de Cuicatlán-Concepción Pápalo, Oaxaca. *Revista Mexicana de Ciencias Geológicas* **7**, 127–35.

**Delgado-Argote LA, López-Martínez M, York D and Hall CM** (1992) Geologic framework and geochronology of ultramafic complexes of southern Mexico. *Canadian Journal of Earth Sciences* **29**, 1590–604. doi: 10.1139/e92-125.

**Donelick RA, O'Sullivan PB and Ketcham RA** (2005) Apatite fission-track analysis. *Reviews in Mineralogy and Geochemistry* **58**, 49–94. doi: 10.2138/rmg.2005.58.3.

**Ducea MN, Valencia VA, Shoemaker S, Reiners PW, DeCelles PG, Campa MF, Morán-Zenteno D and Ruiz J** (2004) Rates of sediment recycling beneath the Acapulco trench: constraints from (U-Th)/He thermochronology. *Journal of Geophysical Research: Solid Earth* **109**, B09404. doi: 10.1029/2004JB003112.

**Elías-Herrera M, Ortega-Gutiérrez F, Sánchez-Zavala JL, Macías-Romo C, Ortega-Rivera A and Iriondo A** (2005) The Caltepec fault: exposed roots of a long-lived tectonic boundary between two continental terranes of southern Mexico. *Boletín de la Sociedad Geológica Mexicana* **57**, 83–109. doi: 10.18268/bsgm2005v57n1a5.

**Espejo-Bautista G, Ortega-Gutiérrez F, Solari LA, Maldonado R and Valencia-Morales YT** (2022) The Sierra de Juárez Complex: a new Gondwanan Neoproterozoic-early Palaeozoic metamorphic terrane in southern Mexico. *International Geology Review* **64**, 631–53. doi: 10.1080/00206814.2020.1870172.

**Estrada-Carmona J, Weber B, Scherer EE, Martens U and Elías-Herrera M** (2016) Lu-Hf geochronology of Mississippian high-pressure metamorphism in the Acatlán Complex, southern México. *Gondwana Research* **34**, 174–86. doi: 10.1016/j.gr.2015.02.016.

**Fitz-Díaz E, Hudleston P, Tolson G and van der Pluijm B** (2014) Progressive, episodic deformation in the Mexican Fold–Thrust Belt (Central Mexico): evidence from isotopic dating of folds and faults. *International Geology Review* **56**, 734–55. doi: 10.1080/00206814.2014.896228.

**Fitz-Díaz E, Lawton T, Juárez-Arriaga E and Chávez-Cabello G** (2018) The Cretaceous-Paleogene Mexican orogen: structure, basin development, magmatism and tectonics. *Earth-Science Reviews* **183**, 56–84. doi: 10.1016/j.earscirev.2017.03.002.

**Fitz-Díaz E, Tolson G, Camprubí A, Rubio-Ramos MA and Prol-Ledesma RM** (2008) Deformación, vetas, inclusiones fluidas y la evolución tectónica de las rocas cretácicas de Valle de Bravo, Estado de México. *Revista Mexicana de Ciencias Geológicas* **25**, 59–81.

**Fitz-Díaz E, Tolson G, Hudleston P, Bolaños-Rodríguez D, Ortega-Flores B and Serrano AV** (2012) The role of folding in the development of the Mexican fold-and-thrust belt. *Geosphere* **8**, 931–49. doi: 10.1130/GES00759.1.

**Flores-Barragán MA, Velasco-de León MP, Lozano-Carmona DE and Ortega-Chavez E** (2019) New paleofloral data from the Matzitzi Formation and their implications for timing of deposition. In *GeoPangea Symposium, Boletín del Instituto de Geología no. 122*, pp. 21–2. Ciudad de México: Instituto de Geología, Universidad Nacional Autónoma de México (in Spanish).

**Garduño-Martínez DE, Pi Puig T, Solé J, Martini M and Alcalá-Martínez JR** (2015) K-Ar illite-mica age constraints on the formation and reactivation history of the El Doctor fault zone, central Mexico. *Revista Mexicana de Ciencias Geológicas* **32**, 306–22.

**Gleadow AJW, Duddy IR, Green PF and Lovering JF** (1986) Confined fission track lengths in apatite: a diagnostic tool for thermal history analysis. *Contributions to Mineralogy and Petrology* **94**, 405–15. doi: 10.1007/BF00376334.

**Gray GG, Pottorf RJ, Yurewicz DA, Mahon KI, Pevear DR and Chuchla RJ** (2001) Thermal and chronological record of syn- to post-Laramide burial and exhumation, Sierra Madre Oriental, Mexico. In *The Western Gulf of Mexico Basin: Tectonics, Sedimentary Basins and Petroleum Systems* (eds C Bartolini, RT Buffler and A Cantú-Chapa), pp. 159–82. American Association of Petroleum Geologists Memoir no. 75. doi: 10.1306/M75768C7.

**Guerrero-Paz DN, Abdullin F, Ortega-Flores B, Solari L, Ortega-Obregón C and Juárez-Arriaga E** (2020) Late Cretaceous to Eocene denudation history of the Tolimán area, southern Sierra Madre Oriental, central Mexico. In *Southern and Central Mexico: Basement Framework, Tectonic Evolution, and Provenance of Mesozoic–Cenozoic Basins* (eds UC Martens and RS Molina Garza), pp. 439–52. Geological Society of America, Special Paper no. 546. doi: 10.1130/2019.2546(18).

**Hasebe N, Barbarand J, Jarvis K, Carter A and Hurford AJ** (2004) Apatite fission-track chronometry using laser ablation ICP-MS. *Chemical Geology* **207**, 135–45. doi: 10.1016/j.chemgeo.2004.01.007.

**Keppie JD, Dostal J and Li J** (2018) Nd isotopic data indicating Oaxacan source of Ordovician granitoids in the Acatlán Complex, southern Mexico: paleogeographic implications. *Tectonophysics* **740**, 1–9. doi: 10.1016/j.tecto.2018.05.004.

**Keppie JD, Dostal J, Murphy JB and Nance RD** (2008) Synthesis and tectonic interpretation of the westernmost Paleozoic Variscan orogen in southern Mexico: from rifted Rheic margin to active Pacific margin. *Tectonophysics* **461**, 277–90. doi: 10.1016/j.tecto.2008.01.012.

**Ketcham RA** (2005) Forward and inverse modeling of low-temperature thermochronometry data. *Reviews in Mineralogy and Geochemistry* **58**, 275–314. doi: 10.2138/rmg.2005.58.11.

**Ketcham RA, Carter A, Donelick RA, Barbarand J and Hurford AJ** (2007) Improved modeling of fission-track annealing in apatite. *American Mineralogist* **92**, 799–810. doi: 10.2138/am.2007.2281.

**Maldonado R, Corona-Chávez P, Solari L, Ortega-Obregón C and Poli S** (2020) Petrology and U–Pb geochronology of high-grade metavolcano-sedimentary rocks from central Xolapa Complex, southern Mexico. *Lithos* **378**, 105802. doi: 10.1016/j.lithos.2020.105802.

**Martini M, Anaya Guarneros JA, Solar L, Bedoya A, Zepeda-Martínez M and Villanueva-Amadoz U** (2022) The Matzitzi Formation in southern Mexico: a record of Pangea final assembly or breakup initiation along inherited suture belts? *Basin Research* **34**, 727–47. doi: 10.1111/bre.12638.

**Martini M and Ortega-Gutiérrez F** (2018) Tectono-stratigraphic evolution of Mexico during the break-up of Pangea: a review. *Earth-Science Reviews* **183**, 38–55. doi: 10.1016/j.earscirev.2016.06.013.

**Martini M, Solari L and López-Martínez M** (2014) Correlating the Arperos Basin from Guanajuato, to Santo Tomás, southern Mexico: implications for the paleogeography and origin of the Guerrero terrain. *Geosphere* **10**, 1385–401. doi: 10.1130/GES01055.1.

**Martini M, Solé J, Garduño-Martínez DE, Puig TP and Omaña L** (2016) Evidence for two Cretaceous superposed orogenic belts in central Mexico based on paleontological and K-Ar geochronological data from the Sierra de los Cuarzos. *Geosphere* **12**, 1257–70. doi: 10.1130/GES01275.1.

**Mendoza-Rosales CC, Centeno-García E, Silva-Romo G, Campos-Madrigal E and Bernal JP** (2010) Barremian rift-related turbidites and alkaline volcanism in southern Mexico and their role in the opening of the Gulf of Mexico. *Earth and Planetary Science Letters* **295**, 419–34. doi: 10.1016/j.epsl.2010.04.020.

**Meneses-Rocha JJ** (2001) Tectonic evolution of the Ixtapa graben, an example of a strike-slip basin of southeastern Mexico: implications for regional petroleum systems. In *The Western Gulf of Mexico Basin: Tectonics, Sedimentary Basins and Petroleum Systems* (eds C Bartolini, RT Buffler and A Cantú-Chapa), pp. 183–216. American Association of Petroleum Geologists Memoir no. 75. doi: 10.1306/M75768C8.

**Nieto-Samaniego AF, Alaniz-Álvarez SA, Silva-Romo G, Eguiza-Castro MH and Mendoza-Rosales CC** (2006) Latest Cretaceous to Miocene deformation events in the Eastern Sierra Madre del Sur, Mexico, inferred from the geometry and age of major structurers. *Geological Society of America Bulletin* **118**, 238–52. doi: 10.1130/B25730.1.

**Ortega-Gutiérrez F** (1978) Estratigrafía del Complejo Acatlán en la Mixteca baja, estados de Puebla y Oaxaca. *Revista del Instituto de Geología* **2**, 112–31.

**Ortega-Gutiérrez F, Elías-Herrera M, Morán-Zenteno DJ, Solari L, Weber B and Luna-González L** (2018) The pre-Mesozoic metamorphic basement of Mexico, 1.5 billion years of crustal evolution. *Earth-Science Reviews* **183**, 2–37. doi: 10.1016/j.earscirev.2018.03.006.

**Ortega-Gutiérrez F, Elías-Herrera M, Reyes-Salas M, Macías-Romo C and López R** (1999). Late Ordovician–Early Silurian continental collisional orogeny in southern Mexico and its bearing on Gondwana-Laurentia connections. *Geology* **27**, 719–22. doi: 10.1130/0091-7613(1999)027<0719:LOESCC>2.3.CO;2.

**Ortega-Obregón C, Abdullin F, Solari L, Schaaf P and Solís-Pichardo G** (2019) Apatite U–Pb dating at UNAM laboratories: analytical protocols and examples of its application. *Revista Mexicana de Ciencias Geológicas* **36**, 27–37. doi: 10.22201/cgeo.20072902e.2019.1.749.

**Padilla y Sánchez RJ** (2007) Evolución geológica del sureste mexicano desde el Mesozoico al presente en el contexto regional del Golfo de México. *Boletín de la Sociedad Geológica Mexicana* **59**, 19–42. doi: 10.18268/BSGM2007v59n1a3.

**Palacios-García NB and Martini M** (2014) From back-arc rifting to arc accretion: the Late Jurassic–Early Cretaceous evolution of the Guerrero terrane recorded by a major provenance change in sandstones from the Sierra de los Cuarzos area, central Mexico. *International Geology Review* **56**, 1377–94. doi: 10.1080/00206814.2014.938367.

**Parolari M, Martini M, Gómez-Tuena A, Ortega-Gutiérrez F, Errázuriz-Henao C and Cavazos-Tovar JG** (2022) The petrogenesis of Early–Middle Jurassic magmatism in southern and central Mexico and its role during the break-up of Western Pangaea. *Geological Magazine* **159**, 873–92. doi: 10.1017/S0016756822000061.

**Paton C, Hellstrom J, Paul B, Woodhead J and Hergt J** (2011) Iolite: freeware for the visualisation and processing of mass spectrometry data. *Journal of Analytical Atomic Spectrometry* **26**, 2508–18. doi: 10.1039/c1ja10172b.

**Pearce NJ, Perkins WT, Westgate JA, Gorton MP, Jackson SE, Neal CR and Chenery SP** (1997) A compilation of new and published major and trace element data for NIST SRM 610 and NIST SRM 612 glass reference materials. *Geostandards and Geoanalytical Research* **21**, 115–44. doi: 10.1111/j.1751-908X.1997.tb00538.x.

**Pérez-Gutiérrez R, Solari LA, Gómez-Tuena A and Valencia VA** (2009) El terreno Cuicateco: ¿cuenca oceánica con influencia de subducción del Cretácico Superior en el sur de México? Nuevos datos estructurales, geoquímicos y geocronológicos. *Revista Mexicana de Ciencias Geológicas* **26**, 222–42.

**Ramírez-Calderón M, Bedoya A, Abdullin F, Martini M, Solari L and Ortega-Obregón C** (2021) Triassic breakup of Pangea in southern Mexico: thermochronological evidence from the Tianguistengo formation. *Geochemistry* **81**, 125776. doi: 10.1016/j.chemer.2021.125776.

**Sedlock RL, Ortega-Gutiérrez F and Speed RC** (1993) *Tectonostratigraphic Terranes and Tectonic Evolution of Mexico*. Geological Society of America, Special Paper vol. 278. doi: 10.1130/SPE278.

**Shchepetilnikova V, Solé J, Solari L and Abdullin F** (2015) A chronological and chemical zircon study of some pegmatite dikes and lenses from the central part (Ayoquezco-Ejutla) of the Oaxacan Complex, southern Mexico. *Revista Mexicana de Ciencias Geológicas* **32**, 123–43.

**Silva A** (1970) Plantas del Pensilvánico de la región de Tehuacan. *Universidad Nacional Autónoma de México, Instituto de Geología, Paleontología Mexicana* **29**, 1–108.

**Solé J and Pi T** (2005) An empirical calibration for $^4$He quantification in minerals and rocks by laser fusion and noble gas mass spectrometry using Cerro de Mercado (Durango, Mexico) fluorapatite as a standard. *Analytica Chimica Acta* **535**, 325–30. doi: 10.1016/j.aca.2004.12.020.

**Talavera-Mendoza O, Ruiz J, Gehrels GE, Meza-Figueroa DM, Vega-Granillo R and Campa-Uranga MF** (2005) U–Pb geochronology of the Acatlán Complex and implications for the Paleozoic paleogeography and tectonic evolution of southern Mexico. *Earth and Planetary Science Letters* **235**, 682–99. doi: 10.1016/j.epsl.2005.04.013.

**van der Meer DG, Spakman W, Van Hinsbergen DJ, Amaru ML and Torsvik TH** (2010) Towards absolute plate motions constrained by lower-mantle slab remnants. *Nature Geoscience* **3**, 36–40. doi: 10.1038/ngeo708.

**Vega-Granillo R, Talavera-Mendoza O, Meza-Figueroa D, Ruiz J, Gehrels GE, López-Martínez M and de la Cruz-Vargas JC** (2007) Pressure-temperature-time evolution of Paleozoic high-pressure rocks of the Acatlán Complex (southern Mexico): implications for the evolution of the Iapetus and Rheic Oceans. *Geological Society of America Bulletin* **119**, 1249–64. doi: 10.1130/B226031.1.

**Vermeesch P** (2009) RadialPlotter: a Java application for fission track, luminescence and other radial plots. *Radiation Measurements* **44**, 409–10. doi: 10.1016/j.radmeas.2009.05.003.

**Vermeesch P** (2017) Statistics for LA-ICP-MS based fission track dating. *Chemical Geology* **456**, 19–27. doi: 10.1016/j.chemgeo.2017.03.002.

**Vermeesch P** (2018) IsoplotR: a free and open toolbox for geochronology. *Geoscience Frontiers* **9**, 1479–93. doi: 10.1016/j.gsf.2018.04.001.

**Weber R** (1997) How old is the Triassic flora of Sonora and Tamaulipas and news on Leonardian floras in Puebla and Hidalgo, Mexico. *Revista Mexicana de Ciencias Geológicas* **14**, 225–43.

**Wilson JL and Ward WC** (1993) Early Cretaceous carbonate platforms of northeastern and east-central Mexico. In *Cretaceous Carbonate Platforms* (eds JA Simo, RW Scott and JP Masse), pp. 35–49. American Association of Petroleum Geologists Memoir no. 56.